

# Binding two and three $\alpha$ particles in cold neutron matter

H. Moriya,<sup>1,\*</sup> H. Tajima,<sup>2,3,†</sup> W. Horiuchi,<sup>1,‡</sup> K. Iida,<sup>3,§</sup> and E. Nakano<sup>3,¶</sup>

<sup>1</sup>*Department of Physics, Hokkaido University, Sapporo 060-0810, Japan*

<sup>2</sup>*Department of Physics, Graduate School of Science,  
The University of Tokyo, Tokyo 113-0033, Japan*

<sup>3</sup>*Department of Mathematics and Physics, Kochi University, Kochi 780-8520, Japan*

(Dated: October 12, 2021)

We elucidate the fate of neighboring two and three  $\alpha$  particles in cold neutron matter by focusing on an analogy between such  $\alpha$  systems and Fermi polarons realized in ultracold atoms. We describe in-medium excitation properties of an  $\alpha$  particle and neutron-mediated two- and three- $\alpha$  interactions using theoretical approaches developed for studies of cold atomic systems. We numerically solve the few-body Schrödinger equation of  $\alpha$  particles within standard  $\alpha$  cluster models combined with in-medium properties of  $\alpha$  particles. We point out that the resultant two- $\alpha$  ground state and three- $\alpha$  first excited state, which correspond to  $^8\text{Be}$  and the Hoyle state, respectively, known as main components in the triple- $\alpha$  reaction, can become bound states in such a many-neutron background although these states are unstable in vacuum. Our results suggest a significance of these in-medium cluster states not only in astrophysical environments such as core-collapsed supernova explosions and neutron star mergers but also in neutron-rich nuclei.

## I. INTRODUCTION

An  $\alpha$  particle ( $^4\text{He}$  nucleus) has a significantly large binding energy compared to other light elements and hence can be an important ingredient in understanding the structure of nuclei as well as the origin of elements. In light  $N = Z$  nuclei, the threshold energy for  $\alpha$  particle disintegration becomes low and even comparable to the one- $\alpha$  separation energy, which helps the  $\alpha$  cluster structure to emerge in the spectrum of such light nuclei as predicted by the Ikeda diagram [1].

One of the most famous examples of the  $\alpha$  cluster structure is the first excited  $J^\pi = 0^+$  state of  $^{12}\text{C}$ , which was originally predicted by Fred Hoyle [2]. This state, which is often called the Hoyle state, is recognized as having a well-developed three- $\alpha$  cluster structure. The existence of such cluster states plays a role in enhancing the reaction rate at extremely low energies near the Gamow window. The  $^{12}\text{C}$  element forms dominantly through a sequential reaction in which a resonant two- $\alpha$  system, the ground state of  $^8\text{Be}$ , absorbs another  $\alpha$  particle via radiative capture process [3]. The accurate description of such  $\alpha$  induced reactions can impact astrophysically important explosive phenomena [4], such as core collapse supernovae and neutron star mergers, which have recently started to be measured through gravitational waves [5].

The importance of  $\alpha$  clusters has extended from light nuclei to many-nucleon systems such as medium-heavy nuclei and nuclear matter. The role of  $\alpha$  particles in supernova explosions has attracted attention [6]. Very recently, an interesting indication that  $\alpha$  clusters emerge in

a surface region of medium-heavy mass nuclei have been obtained by a systematic measurement via the  $\alpha$  knock-out reactions [7]. These encourage us to study the formation and structure of an  $\alpha$  particle in dilute neutron-rich matter. In Ref. [8], three of the present authors (E.N., K.I., and W.H.) discussed the static properties of an  $\alpha$  particle in cold dilute neutron matter. The effective mass of the in-medium  $\alpha$  particle is enhanced by the interaction with the neutron matter, implying the possibility of binding the ground state resonance of  $^8\text{Be}$  and the Hoyle state in such an extreme environment. If realized, these molecular-like ‘bound’ states will take part in the astrophysical reactions, in addition to compact multi- $\alpha$  cluster systems, e.g., the ground states of  $^{12}\text{C}$  and  $^{16}\text{O}$ , and thus should be incorporated explicitly as ingredients of simulations of astrophysical nuclear processes [9], which may affect the local abundance of the chemical elements.

In general, it is challenging to see how impurity particles behave in many-body backgrounds like a Fermi sea due to infinitely large degrees of freedom. Nevertheless, this problem has been tackled in ultracold atoms theoretically and experimentally in terms of Fermi polarons [10–12]; an impurity atom is dressed by excitations of majority Fermi atoms via interspecies interactions. Quasiparticle properties of a single polaron such as the effective mass have precisely been measured in experiments [13–21] and successfully described by various theoretical frameworks such as a variational method [22] and a  $T$ -matrix approximation [23]. Moreover, fermion-mediated interactions between polarons have also been observed experimentally [24, 25].

In this work, we investigate the structure of two- and three- $\alpha$  systems in dilute neutron matter of density lower than about  $1/100$  of the saturation density  $\sim 0.01\rho_0$  at zero temperature and discuss their medium-induced stabilization by regarding each  $\alpha$  particle as a mobile impurity immersed in the neutron medium. Analogy with Fermi polarons realized in ultracold atoms allows us to

\* moriya@nucl.sci.hokudai.ac.jp

† hiroyuki.tajima@phys.s.u-tokyo.ac.jp

‡ whoriuchi@nucl.sci.hokudai.ac.jp

§ iida@kochi-u.ac.jp

¶ e.nakano@kochi-u.ac.jp

utilize the results obtained for quasiparticle properties of a single  $\alpha$  particle in neutron matter [8] by using Chevy's variational ansatz known to give a quantitative description of Fermi atomic polarons. To discuss the stability of two- and three- $\alpha$  particles immersed in neutron matter, moreover, we derive medium-induced two- and three-body interactions among polarons using a diagrammatic approach. Once the effective Hamiltonian is set, the structure of the in-medium two- and three- $\alpha$  systems can be accurately obtained from the solution of the corresponding few-body Schrödinger equation. This study offers the first quantitative evaluation of the energy and the pair density distribution of two and three- $\alpha$  systems in cold neutron matter.

This paper is organized as follows. The next section describes models of the in-medium multi- $\alpha$  systems. Section II A is devoted to the derivation of induced two- and three- $\alpha$  interactions in a neutron Fermi sea. Section II B gives the effective Hamiltonian for the multi- $\alpha$  systems in the cold neutron matter. The two cluster models employed in this study are briefly described in Sec. II C. Given the effective Hamiltonian, in Sec. II D, we address how to solve the few- $\alpha$  Schrödinger equation precisely using the correlated Gaussian expansion. Section III presents our results. The possibility of the medium-induced stabilization of the two- and three- $\alpha$  systems is discussed. The conclusion and future prospects are given in Sec. IV.

## II. MODELS OF IN-MEDIUM TWO- AND THREE- $\alpha$ SYSTEMS

Let us proceed to construct models for the systems of two and three  $\alpha$  particles of bare mass  $M$  in a dilute gas of neutrons of bare mass  $m$  at zero temperature. Since we are interested in  $\alpha$  particles in astrophysical environments where the temperature is higher than the neutron superfluid critical temperature [4], we can safely assume that the neutron gas is in a normal state. We are interested in astrophysical situations where  $\alpha$  particles occur thermally rather than by external factors; hence, the crust of very cold neutron stars is out of our scope. We also ignore the neutron-neutron interaction for simplicity. Although we employ the zero-temperature results for the induced interactions among  $\alpha$  particles and the  $\alpha$  effective mass as will be discussed below, such zero-temperature treatment can be justified when the temperature is below both the neutron Fermi temperature  $T_F = \frac{\hbar^2 k_F^2}{2mk_B}$  and the cutoff energy scale  $\frac{\hbar^2}{m_r r_0^2} \simeq 25$  MeV of the neutron- $\alpha$  interaction with the effective range  $r_0 = 1.43$  fm [8]. We finally remark that at sufficiently high neutron densities corresponding to  $k_F \gtrsim 0.3$  fm $^{-1}$ , a  $p$ -wave resonance ( $^5\text{He}$ ) could be stabilized by the Pauli blocking effect and emerge as a nuclear ingredient [8, 9]. This possibility is another issue to be tackled with, but is beyond the scope of this work.

### A. Derivation of induced two- and three-body interactions in cold neutron matter

We start with diagrammatic derivation of the medium-induced two- and three-body interactions among  $\alpha$  particles in a neutron Fermi sea. As depicted diagrammatically in Fig. 1(a), the induced two-body interaction between two  $\alpha$  particles can be obtained up to leading order in  $a$  as [26]

$$V_{\text{eff}}^{(2)}(\mathbf{q}, i\nu_\ell) = - \left( \frac{2\pi\hbar^2 a}{m_r} \right)^2 \times \frac{k_B T}{\hbar^2} \sum_{\sigma=\uparrow, \downarrow} \sum_{\mathbf{p}, \omega_n} G_\sigma(\mathbf{p} + \mathbf{q}, i\omega_n + i\nu_\ell) G_\sigma(\mathbf{p}, i\omega_n), \quad (1)$$

where  $k_B$  is the Boltzmann constant,  $(\mathbf{q}, i\nu_\ell) = (\mathbf{k} - \mathbf{k}', i\nu_s - i\nu_{s'})$  is the transferred four-momentum,  $\nu_\ell = 2\ell\pi k_B T/\hbar$  is the bosonic Matsubara frequency [27],  $G_\sigma(\mathbf{p}, i\omega_n) = (i\omega_n - \xi_{\mathbf{p}}/\hbar)^{-1}$  is the thermal Green's function of a neutron with energy  $\xi_{\mathbf{p}} = \frac{p^2}{2m} - \varepsilon_F$  relative to the neutron Fermi energy  $\varepsilon_F$ , and  $m_r = (m^{-1} + M^{-1})^{-1}$  is the reduced mass.  $a = 2.64$  fm is the  $s$ -wave neutron- $\alpha$  scattering length [8]. Taking the summation of the fermionic Matsubara frequency  $\omega_n = (2n+1)\pi k_B T/\hbar$  [27], we obtain the induced two-body interaction as

$$V_{\text{eff}}^{(2)}(\mathbf{q}, i\nu_\ell) = 2 \left( \frac{2\pi\hbar^2 a}{m_r} \right)^2 \sum_{\mathbf{p}} \frac{f(\xi_{\mathbf{p}}) - f(\xi_{\mathbf{p}+\mathbf{q}})}{i\hbar\nu_\ell + \xi_{\mathbf{p}} - \xi_{\mathbf{p}+\mathbf{q}}}. \quad (2)$$

In the low-energy limit  $\nu_\ell = 0$  at  $T = 0$ , Eq. (2) reduces to

$$V_{\text{eff}}^{(2)}(\mathbf{q}, 0) = - \frac{mk_F}{2\pi^2\hbar^2} \left( \frac{2\pi\hbar^2 a}{m_r} \right)^2 \times \left[ 1 + \frac{k_F}{q} \left( 1 - \frac{q^2}{4k_F^2} \right) \ln \left| \frac{q + 2k_F}{q - 2k_F} \right| \right]. \quad (3)$$

Note that in the long wavelength limit ( $\mathbf{q} \rightarrow 0$ ), Eq. (3) can be expressed by the compressibility  $\kappa = \frac{1}{\rho^2} \left( \frac{\partial \rho}{\partial \mu} \right)$  of neutron matter as  $V_{\text{eff}}^{(2)}(\mathbf{q} \rightarrow \mathbf{0}, 0) = - \left( \frac{2\pi\hbar^2 a}{m_r} \right)^2 \rho^2 \kappa$ . By taking the inverse Fourier transformation of Eq. (3), we obtain the well-known Ruderman-Kittel-Kasuya-Yosida (RKKY) form of the induced two-body interaction in the coordinate space as [28–32]

$$V_{\text{eff}}^{(2)}(\mathbf{r}_1, \mathbf{r}_2) = \frac{m}{8\pi^3\hbar^2} \left( \frac{2\pi\hbar^2 a}{m_r} \right)^2 \times \frac{(2k_F r) \cos(2k_F r) - \sin(2k_F r)}{r^4}, \quad (4)$$

where  $r = |\mathbf{r}_1 - \mathbf{r}_2|$ .

Moreover, as diagrammatically drawn in Fig. 1(b), the induced three-body interaction up to leading order in  $a$

is given by [33]

$$\begin{aligned}
V_{\text{eff}}^{(3)}(\mathbf{k}, \mathbf{q}, i\nu_\ell, i\nu_u) &= 2 \left( \frac{2\pi\hbar^2 a}{m_r} \right)^3 \\
&\times \frac{k_B T}{\hbar^3} \sum_{\sigma=\uparrow, \downarrow} \sum_{\mathbf{p}, \omega_n} G_\sigma(\mathbf{p}, i\omega_n) G_\sigma(\mathbf{p} + \mathbf{k} + \mathbf{q}/2, i\omega_n + i\nu_\ell) \\
&\times G_\sigma(\mathbf{p} + \mathbf{k} - \mathbf{q}/2, i\omega_n + i\nu_\ell - i\nu_u), \quad (5)
\end{aligned}$$

where  $\mathbf{k} = \mathbf{k}_1 - \mathbf{k}_2$ ,  $\mathbf{q} = \mathbf{q}_1 - \mathbf{q}_2$ ,  $i\nu_\ell = i\nu_{s_1} - i\nu_{s_2}$ , and  $i\nu_u = i\nu_{j_1} - i\nu_{j_2}$  are the transferred four-momenta. In the low-energy limit ( $i\nu_\ell = i\nu_u = 0$ ), the induced three-body interaction in the coordinate space can be obtained as

$$V_{\text{eff}}^{(3)}(\mathbf{r}_1, \mathbf{r}_2, \mathbf{r}_3) = \sum_{\mathbf{k}, \mathbf{q}} V_{\text{eff}}^{(3)}(\mathbf{k}, \mathbf{q}, 0, 0) e^{-i\mathbf{k}\cdot\mathbf{x}_1 + i\mathbf{q}\cdot\mathbf{x}_2}, \quad (6)$$

where  $\mathbf{x}_1 = \mathbf{r}_1 - \mathbf{r}_2$  and  $\mathbf{x}_2 = \mathbf{r}_3 - (\mathbf{r}_1 + \mathbf{r}_2)/2$ . For simplicity, we employ the contact-type three-body interaction whose coupling constant is given by

$$\begin{aligned}
V_{\text{eff}}^{(3)}(\mathbf{0}, \mathbf{0}, 0, 0) &= 2 \left( \frac{2\pi\hbar^2 a}{m_r} \right)^3 \frac{k_B T}{\hbar^3} \sum_{\sigma} \sum_{\mathbf{p}, \omega_n} [G_\sigma(\mathbf{p}, i\omega_n)]^3 \\
&= \frac{m^2}{\pi^2 \hbar^4 k_F} \left( \frac{2\pi\hbar^2 a}{m_r} \right)^3. \quad (7)
\end{aligned}$$

Thus, we obtain

$$V_{\text{eff}}^{(3)}(\mathbf{r}_1, \mathbf{r}_2, \mathbf{r}_3) = \frac{m^2}{\pi^2 \hbar^4 k_F} \left( \frac{2\pi\hbar^2 a}{m_r} \right)^3 \delta(\mathbf{x}_1) \delta(\mathbf{x}_2). \quad (8)$$

Note that to adopt the contact interaction (8) is equivalent to the local density approximation.

### B. Hamiltonian for two- and three- $\alpha$ particles in cold neutron matter

A single  $\alpha$  particle immersed in cold neutron matter has its mass  $M$  changed into the effective mass  $M^*$  by the interaction with neutrons in the medium. This particle, dressed with neutron excitations, can be regarded as a polaron. As a natural extension of the previous study on this polaron [8], we consider two- and three- $\alpha$  systems immersed in cold neutron matter. As we shall see, the mass enhancement through  $M^*$  acts to increase binding of these systems. The explicit form of the Hamiltonian of the three- $\alpha$  system in cold neutron matter is

$$\begin{aligned}
H &= \sum_{i=1}^3 \frac{\mathbf{p}_i^2}{2M^*} - T_{\text{cm}} \\
&+ \sum_{i<j=1}^3 \left[ U_{ij}^{(2)} + V_{\text{eff};ij}^{(2)} \right] + U^{(3)} + V_{\text{eff}}^{(3)}, \quad (9)
\end{aligned}$$

where the center-of-mass kinetic energy term  $T_{\text{cm}}$  is subtracted,  $U^{(x)}$  ( $x = 2, 3$ ) denotes the  $x\alpha$  potential in vacuum including the Coulomb term, and  $V_{\text{eff}}^{(x)}$  is the induced  $x\alpha$  interaction in the neutron medium with the

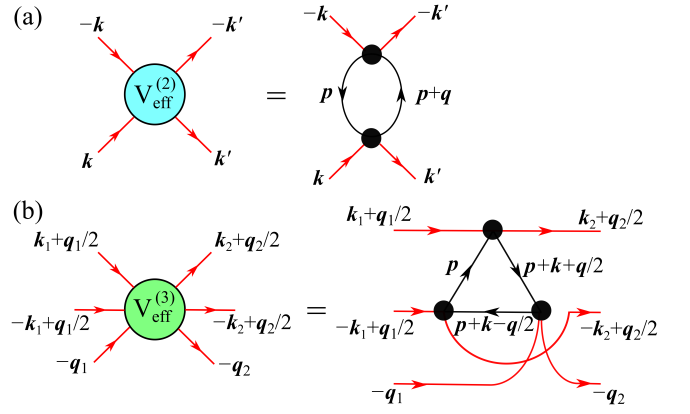


FIG. 1. Feynman diagrams in the center-of-mass frame of  $\alpha$  particles that represent the induced (a) two-body interaction  $V_{\text{eff}}^{(2)}(\mathbf{q}, i\nu_\ell)$  and (b) three-body interaction  $V_{\text{eff}}^{(3)}(\mathbf{k}, \mathbf{q}, i\nu_\ell, i\nu_u)$  among  $\alpha$  particles immersed in neutron matter. For  $V_{\text{eff}}^{(2)}(\mathbf{q}, i\nu_\ell)$ , the incoming (outgoing) momenta of  $\alpha$  particles are given by  $\mathbf{k}$  and  $-\mathbf{k}$  ( $\mathbf{k}'$  and  $-\mathbf{k}'$ ). For  $V_{\text{eff}}^{(3)}(\mathbf{k}, \mathbf{q}, i\nu_\ell, i\nu_u)$ , the incoming (outgoing) momenta of  $\alpha$  particles are given by  $\mathbf{k}_1 + \mathbf{q}_1/2$ ,  $-\mathbf{k}_1 + \mathbf{q}_1/2$ , and  $-\mathbf{q}_1$  ( $\mathbf{k}_2 + \mathbf{q}_2/2$ ,  $-\mathbf{k}_2 + \mathbf{q}_2/2$ , and  $-\mathbf{q}_2$ ). The internal solid lines denote the thermal Green's function of a neutron.

Fermi momentum  $k_F$ . Note that  $M^*$  and  $V_{\text{eff}}^{(x)}$  depend on  $k_F$ . The  $k_F$  dependence of  $M^*/M$  is taken from Ref. [8]. We take the neutron mass as  $\hbar^2/m = 41.47 \text{ MeV fm}^2$  and  $M = 4m$  to keep the consistency of the parameters given in Ref. [8].

Here we incorporate  $V_{\text{eff}}^{(2)}$  and  $V_{\text{eff}}^{(3)}$  derived in the previous subsection into the Hamiltonian. The original RKKY potential (4) behaves as  $\sim r^{-1}$  at small  $r$  and hence has a singularity at the origin. This is regularized by folding the harmonic oscillator type form factor of the  $\alpha$  particle associated with the nuclear force,  $\left(\frac{8\nu}{3\pi}\right)^{\frac{3}{2}} e^{-\frac{8}{3}\nu u^2}$ , which leads to

$$V_{\text{eff}}^{(2)}(r) = V_{\text{RKKY}}(r) \text{erf}\left(\frac{4}{3}\sqrt{\nu}r\right), \quad (10)$$

where  $\nu$  is also taken as  $0.2675 \text{ fm}^{-2}$  in a way that is consistent with the width parameter of the  $\alpha$  particle [55]. Note that this range is shorter than the  $\alpha$ - $n$  scattering length  $a$  and  $1/k_F$  considered in this work. It is reasonable to take the range of the induced three-body force as the same as the one for the induced two- $\alpha$  interaction, which leads to

$$V_{\text{eff}}^{(3)}(R) = \frac{m^2}{\pi^2 \hbar^4 k_F} \left( \frac{2\pi\hbar^2 a}{m_r} \right)^3 N_\nu e^{-\frac{16}{9}\nu R^2} \quad (11)$$

with the normalization constant of the form factor  $N_\nu = \left(\frac{16\nu}{3\pi}\right)^3$ . Note that  $R^2 = (\mathbf{r}_1 - \mathbf{r}_2)^2 + (\mathbf{r}_2 - \mathbf{r}_3)^2 + (\mathbf{r}_3 - \mathbf{r}_1)^2 = \frac{3}{2}x_1^2 + 2x_2^2$ , which is symmetric in any particle exchange. Since  $a$  is positive, the induced three- $\alpha$  potential

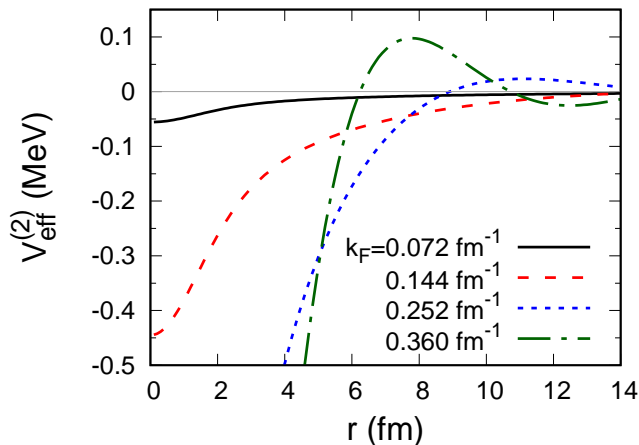


FIG. 2. Induced two-body interaction  $V_{\text{eff}}^{(2)}(r)$  as a function of the  $\alpha$ - $\alpha$  distance  $r$  for various values of the Fermi momenta  $k_F$  of cold neutron matter. The thin horizontal line indicates zero.

is always repulsive; its strength is inversely proportional to  $k_F$ .

Figure 2 plots the  $k_F$  dependence of the induced two- $\alpha$  potential, Eq. (10). At short distances, this two- $\alpha$  interaction is attractive, leading to more stability of multi- $\alpha$  systems. The range of such attraction increases with  $k_F$ , while, for sufficiently large  $k_F$ , some oscillatory behavior appears, a feature reflecting the Friedel oscillation associated with the presence of the neutron Fermi surface. The induced three- $\alpha$  interaction, on the other hand, is repulsive and weakens as  $k_F$  increases. The optimal stability of the three- $\alpha$  system can thus be realized at a certain  $k_F$  that is determined in balance with the purely repulsive induced three- $\alpha$  potential.

The difference of the effective mass from the bare mass, together with the induced interactions, can crucially affect the relative motion between  $\alpha$  particles. In this work, we consider each  $\alpha$  particle to be a structureless particle but treats the Pauli principle in the interaction between  $\alpha$  particles in two different ways. Both potential models well reproduce the empirical  $\alpha$ - $\alpha$  scattering phase shift. Although it is difficult to obtain empirical information on the closest motion, they are known to give different results for the internal region of the relative wave function. See, e.g., [34–36] for some examples in light cluster systems. We utilize such two potential models to evaluate the uncertainty that comes from model choice.

### C. Multi- $\alpha$ cluster models

We start with a standard type of  $\alpha$  cluster model that assumes a shallow and repulsive potential. As  $U^{(2)}$ , we employ the Ali-Bodmer (AB) potential [37] (Set  $a'$  [38]), which reproduces the  $\alpha$ - $\alpha$  scattering phase shift and produces the  $s$ -wave  ${}^8\text{Be}$  ( $0_1^+$ ) resonance position with 0.093

MeV, a value close to the empirical one 0.092 MeV [39]. Note that we get 0.086 MeV in the present calculation because of the use of the different mass parameter of an  $\alpha$  particle ( $M = 4m$ ). The AB potential is  $l$ -dependent and its explicit form is

$$U_{\text{AB}}(r) = \left(125\hat{P}_{l=0} + 20\hat{P}_{l=2}\right) \exp\left(-\frac{r^2}{1.53^2}\right) - 30.18 \exp\left(-\frac{r^2}{2.85^2}\right), \quad (12)$$

where the energy and length are given in units of MeV and fm, and  $\hat{P}_l$  is the projection operator onto the relative angular momentum  $l$ . This potential is so shallow that no bound state appears. The Pauli principle in the interaction between  $\alpha$  particles is simulated by the first repulsive term of the potential. It is known that the empirical energies of states close to the threshold energy of the three- $\alpha$  system are not well reproduced by the two-body interaction alone [40]. Then, one often introduces a phenomenological three- $\alpha$  potential as  $U^{(3)}$ , which only has a single Gaussian attractive term [41]. Because of such simplicity, a similar sort of potential model has often been used to describe astrophysically important reactions [41–47]. This three- $\alpha$  interaction, together with the two- $\alpha$  one, leads to the Hoyle state energy of 0.38 MeV with respect to the three- $\alpha$  threshold, which perfectly agrees with the empirical Hoyle state energy [48].

Another standard cluster model employs a deep attractive potential, which accommodates three redundant bound states  $\phi_{n_f l_f m_f}$  with  $(n_f, l_f) = (0, 0), (1, 0), (0, 2)$  that are forbidden by the Pauli principle in the interaction between two  $\alpha$  particles. When the two- and three- $\alpha$  equations are solved, the orthogonality condition to be imposed for an  $N$ - $\alpha$  system reads

$$\sum_{i < j = 1}^N \sum_{nlm \in f} |\langle \phi_{nlm}(ij) | \Psi \rangle|^2 = 0, \quad (13)$$

where  $f$  and  $\Psi$  denote the Pauli forbidden two- $\alpha$  bound states and the eigenstate of the system, respectively. That is why this kind of model is called the orthogonality condition model (OCM) [49–51], which has often been used as an alternative to the microscopic cluster model and been successful in describing the  $\alpha$  condensed states predicted for  ${}^{12}\text{C}$  and  ${}^{16}\text{O}$  [52, 53]. As demonstrated in Ref. [54], the low energy  $\alpha$ - $\alpha$  scattering phase shifts are well reproduced without introducing repulsive components explicitly in the potential. The relative wave function thus shows a nodal behavior in the internal region.

In the present study, we employ a folding-type two- $\alpha$  potential that was based on the effective nucleon-nucleon interaction [54] and readjusted in Ref. [55]. This potential is expressed in a single Gaussian form that only includes attractive term. The calculated energy of  ${}^8\text{Be}$  is 0.095 MeV, reproducing the empirical energy. The ex-



PLICIT form of the potential is a simple Gaussian form:

$$U_{\text{OCM}}(r) = -106.1 \exp\left(-\frac{r^2}{2.23^2}\right). \quad (14)$$

This potential is apparently much deeper than the AB potential of Eq. (12), and produces the three redundant forbidden states, which should be removed from all the pairwise wave functions in the three- $\alpha$  systems. The present Hamiltonian makes the ground- and Hoyle states overbound only with the two- $\alpha$  interaction, and hence a repulsive phenomenological three- $\alpha$  potential is often introduced to adjust these energies to the empirical values. Some applications with this potential set are given in Refs. [56–58]. Because the calculated Hoyle state energy amounts to no less than 0.78 MeV, here we newly parametrize a three- $\alpha$  potential better able to reproduce the empirical Hoyle state energy 0.38 MeV [48] for a fair comparison with the AB result. The explicit form of the potential in MeV is

$$U^{(3)}(R) = 77.0 \exp(-0.12R^2) - 10.0 \exp(-0.03R^2). \quad (15)$$

The calculated Hoyle state energy is 0.34 MeV, which is close to the empirical energy of the Hoyle state.

#### D. Correlated Gaussian expansion

Let us proceed to construct the wave function of the  $N$ - $\alpha$  system, which is expanded by a superposition of symmetrized correlated Gaussian basis functions [59–61]

$$\Psi^{(k)} = \sum_{i=1}^K C_i^{(k)} \bar{G}(A_i, \mathbf{x}) \quad (16)$$

$$= \sum_{i=1}^K C_i^{(k)} \mathcal{S} \exp\left(-\frac{1}{2} \tilde{\mathbf{x}} A_i \mathbf{x}\right), \quad (17)$$

where  $\mathcal{S}$  denotes the symmetrizer that ensures the symmetry of an identical bosonic system,  $\mathbf{x}$  is the  $(N-1)$ -dimensional column vector composed of a set of the Jacobi coordinate excluding the center-of-mass coordinate  $\mathbf{x}_N$ , and the tilde denotes the transpose of the corresponding matrix. A set of the coefficients  $C_i^{(k)}$  can be obtained by solving the generalized eigenvalue problem

$$\sum_{j=1}^K H_{ij} C_j^{(k)} = E^{(k)} \sum_{j=1}^K B_{ij} C_j^{(k)}, \quad (18)$$

where

$$H_{ij} = \langle \bar{G}(A_i, \mathbf{x}) | H | \bar{G}(A_j, \mathbf{x}) \rangle \quad (19)$$

and

$$B_{ij} = \langle \bar{G}(A_i, \mathbf{x}) | \bar{G}(A_j, \mathbf{x}) \rangle. \quad (20)$$

The nonlinear variational parameter  $A_i$  is a positive definite symmetric  $(N-1)$ -dimensional matrix. Note that its off-diagonal elements, which control correlations among particles, are determined by means of the stochastic variational method [59, 60]. We follow the setup of Ref. [46] to optimize the wave function for the three- $\alpha$  system. The bound state approximation is applied to the positive energy state, which is valid for a state with a narrow decay width [62–64]. The correlated Gaussian approach is flexible enough to describe both short-range and long-range correlations required in this study. See [65, 66] for typical examples that show the power of this approach.

When we incorporate the deep potential model into the calculations, we impose the orthogonality condition practically by using the projection method [67] that adds the pseudo potential or projection operator,

$$\gamma \sum_{i < j = 1}^N \sum_{nlm \in f} |\phi_{nlm}(ij)\rangle \langle \phi_{nlm}(ij)|, \quad (21)$$

to the Hamiltonian. One can eliminate the forbidden states variationally by taking a large  $\gamma$  value. Here, we adopt the harmonic-oscillator wave functions with the width parameter  $\nu = 0.2675 \text{ fm}^{-2}$  [55], which reproduces the size of the  $\alpha$  particle, as the forbidden states to be eliminated from the relative motion between the  $\alpha$  particles. We take  $\gamma = 10^5 \text{ MeV}$  and confirm that the converged wave functions typically contain the forbidden state component of relative magnitude  $\approx 10^{-6}$ .

### III. RESULTS AND DISCUSSIONS

In neutron matter, the effective mass  $M^*$  of an  $\alpha$  particle as well as the induced two- and three- $\alpha$  interactions, changes with  $k_F$  [8]. Here we discuss the influence of these medium effects on the binding energy of the two- and three- $\alpha$  systems. More specifically, we analyze the ground state of the two- $\alpha$  system, i.e.,  ${}^8\text{Be}$ , and the first excited state of the three- $\alpha$  system, i.e., the Hoyle state of  ${}^{12}\text{C}$ , both of which exhibit a resonance in vacuum. We shall show that both the  ${}^8\text{Be}$  and Hoyle states become bound in the neutron medium of sufficiently large  $k_F$ .

Figure 3 shows the energies of the three- $\alpha$  systems relative to the three- $\alpha$  threshold, calculated for AB and OCM as a function of the Fermi momentum of the neutron medium  $k_F$ . To see the contributions of the induced interactions, we compare the energies including the two-body and/or three-body induced interactions with the one in the absence of the induced interactions. In general, each energy thus calculated gains as  $k_F$  increases except for the Hoyle state energies only with  $M^*$  for AB. Note that  $M^*$  increases with  $k_F$  [8], leading to further localization near the potential minima. In fact, the results only with  $M^*$  contribution clearly reflect the properties that the OCM potential only have an attractive component while the AB potential has repulsive and attractive

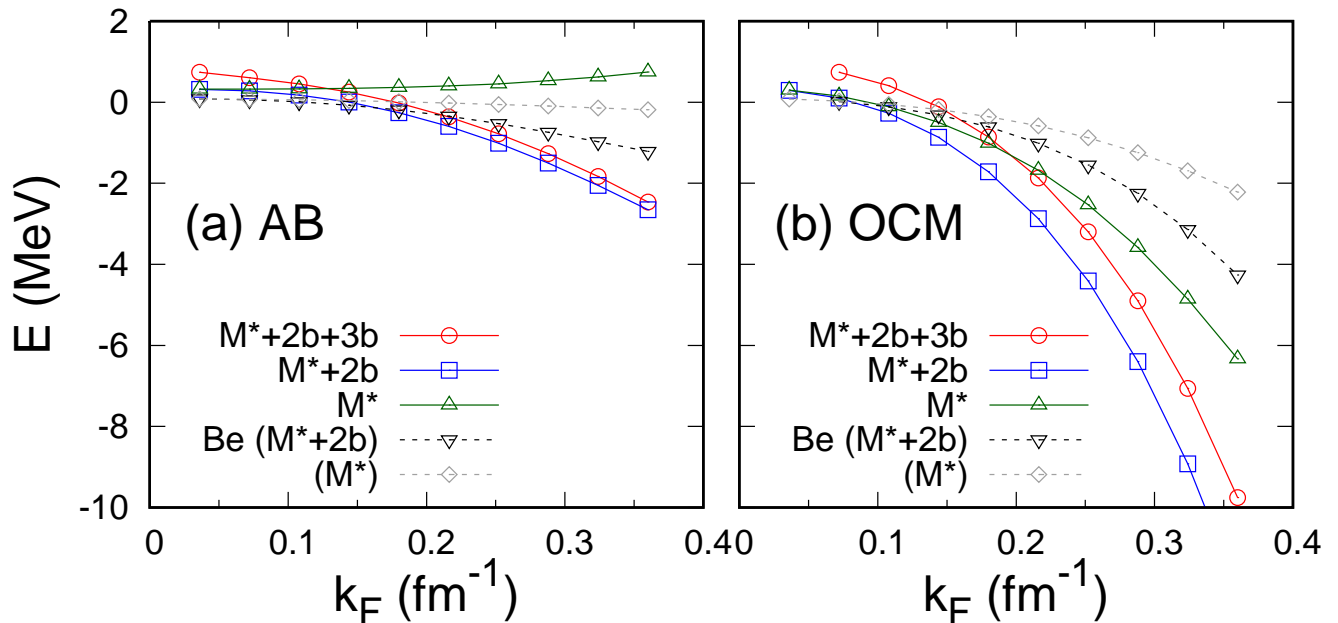


FIG. 3. Energies of the three- $\alpha$  system in neutron matter calculated as a function of the neutron Fermi momentum with different potential models, (a) AB and (b) OCM. The calculations including the effective mass alone as medium effects are denoted by  $M^*$ , while those additionally including the induced two-body force and also the induced three-body force are denoted by  $M^* + 2b$  and  $M^* + 2b + 3b$ , respectively. The results for the two- $\alpha$  system ( ${}^8\text{Be}$ ) are also plotted for comparison. The lines are guide for the eye.

components at short and intermediate distances, respectively.

For the same reason,  $\alpha$  particles of larger  $M^*$  come closer to each other once the induced two- $\alpha$  interaction, which is attractive at short distances as shown in Fig. 2, is taken into account. Then, the induced two-body interaction always plays a role in gaining the binding energy, which can be seen in the results allowing for the induced two-body interaction ( $M^* + 2b$ ). This is consistent with a microscopic  $\alpha + \alpha + n$  cluster model calculation [68], which shows that the  $\alpha$ - $\alpha$  distance shrinks in  ${}^9\text{Be}$  owing to the interaction from the intervening neutron. On the other hand, the induced three- $\alpha$  interaction is always repulsive, which leads to increase in the energy denoted by  $M^* + 2b + 3b$  as compared with the one denoted by  $M^* + 2b$ . The result of OCM ( $M^* + 2b + 3b$ ) with  $k_F = 0.036 \text{ fm}^{-1}$  is not shown because no physically stable state is obtained due to too strong repulsion of the induced three- $\alpha$  interaction.

While all the above-mentioned tendencies apply to the two cluster models, quantitative details look very different. For AB, virtually no contribution from the induced three-body interaction is found because there is only a negligible wave function amplitude in the internal region due to the repulsive component of the AB potential, which will be shown in the next paragraph. The ground state of  ${}^8\text{Be}$  become bound at  $k_F \gtrsim 0.11 \text{ fm}^{-1}$  for AB and  $\gtrsim 0.08 \text{ fm}^{-1}$  for OCM. The Hoyle state becomes bound, i.e., the energy is located below the  ${}^8\text{Be}$  energy, at

$k_F \gtrsim 0.22 \text{ fm}^{-1}$  for AB and  $\gtrsim 0.16 \text{ fm}^{-1}$  for OCM. In the OCM case, the condition for binding of the Hoyle state is determined by a subtle competition between the attractive and repulsive contributions from the induced two- and three-body interactions, respectively. Incidentally, one can safely ignore the excited states and dissociation of an  $\alpha$  particle because the excitation energy to the first excited state in vacuum is far larger than the neutron Fermi energy at neutron densities of interest here. Also, we ignore possible increase in the kinetic energy of the two- and three- $\alpha$  systems due to the Pauli blocking effect, which, in the case of dissolution of  $\alpha$  clusters, would become significant when the density of the nuclear medium exceeds  $0.03 \text{ fm}^{-3}$  [9], again far higher than the medium density considered in this work. Although the binding energy of an  $\alpha$  particle in such a low density medium as considered here can be shifted by several MeV [69], the formation of the molecular-like states near the threshold has yet to be affected significantly because the threshold energy is also shifted by about the same amount. We remark in passing that the polaronic quasiparticle energy, which is typically of order MeV [8], acts as a shift of the binding energy of an  $\alpha$  particle, but does not affect the formation of weakly bound molecular-like states because the threshold energy equally shifts.

This model dependence of the system energy comes from the difference of the internal structure of the relative wave function between  $\alpha$  clusters. To see such difference explicitly we calculate the pair density distributions

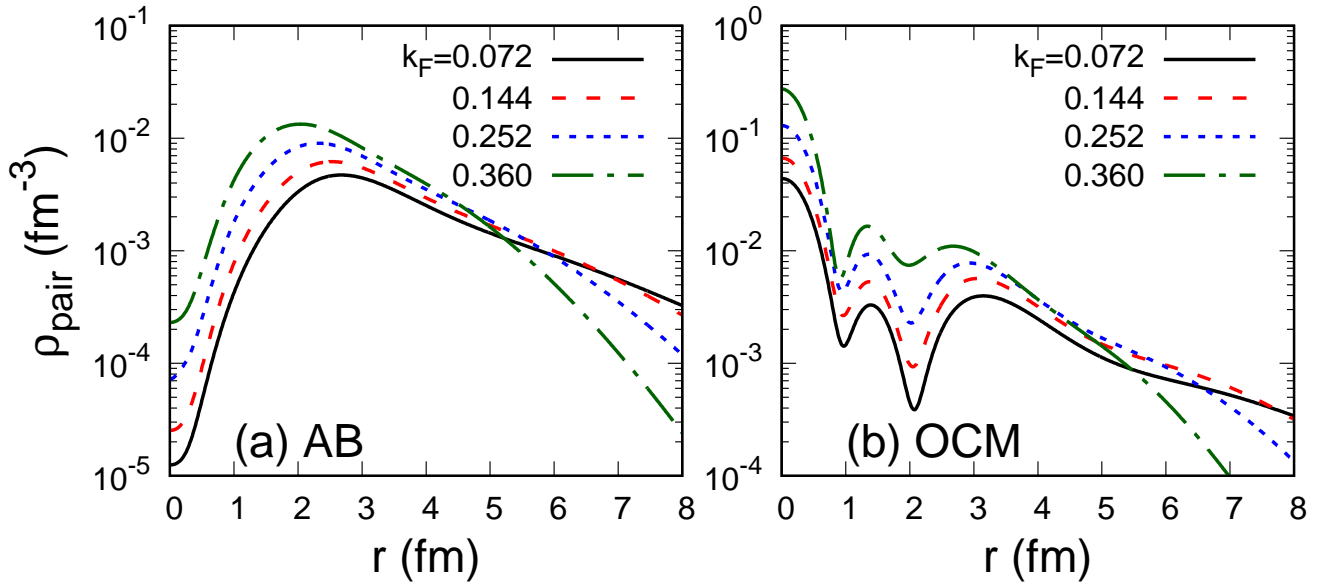


FIG. 4. Pair density distributions  $\rho_{\text{pair}}(r)$  of the three- $\alpha$  system in cold neutron matter of various  $k_F$  with (a) AB and (b) OCM.

defined by

$$\rho_{\text{pair}}(r) = \left\langle \frac{\delta(|\mathbf{r}_1 - \mathbf{r}_2| - r)}{4\pi r^2} \right\rangle, \quad (22)$$

where the bracket denotes the expectation value with the first excited state wave function of the three- $\alpha$  system and  $4\pi \int_0^\infty r^2 \rho_{\text{pair}}(r) dr = 1$ . Figure 4 compares the results for the pair density distribution obtained at various  $k_F$ . For AB, the amplitude of the wave function is strongly suppressed due to the repulsive potential component at short distances,  $\lesssim 2$  fm, while the peak of the amplitude, located near the potential minimum that arises from  $U^{(3)}$ , naturally increases with  $k_F$  or  $M^*$ . In the OCM results, on the other hand, an oscillatory behavior is found at distances  $\lesssim 3$  fm due to the orthogonality condition to the Pauli forbidden states. Since a significant amount of amplitude is present in such an internal region, the wave function in this region is strongly modified as the Hamiltonian changes. For larger  $k_F$  or  $M^*$ , the amplitude of the internal wave function becomes larger, which is natural considering that heavier  $\alpha$  particles are more difficult to move near the OCM potential minimum of zero separation.

We conclude this section by examining how the difference in the pair density distribution between AB and OCM is reflected in the expectation values of the Hamiltonian terms. Figure 5 displays decomposition of the total energy into the contributions of the kinetic, direct interaction, and induced interaction terms. Since the OCM wave function has its internal amplitude disturbed drastically by the medium, the expectation value of the kinetic energy rapidly increases as the  $k_F$  increases for OCM, as can be seen from Fig. 5 (a). This energy cost is dominated by the energy gain from the direct term

$\langle \sum_{ij} U_{ij}^{(2)} + U^{(3)} \rangle$  as plotted in Fig. 5 (b), which is in turn controlled by the two-body OCM potential responsible for the zero-separation potential minimum. For the AB model, the same kind of behavior of both terms occurs, but the medium effects are suppressed due to the repulsive nature of the AB potential at short distances. Finally, Fig. 5 (c) compares the sum of the expectation values from the induced two- and three-body interactions  $\langle \sum_{ij} V_{\text{eff};ij}^{(2)} + V_{\text{eff}}^{(3)} \rangle$  (denoted by  $V_{\text{ind}}$ ) between AB and OCM. In either case, the contribution of the induced three-body force is about one or two orders of magnitude smaller than that of the induced two-body force. The model dependence of the induced interaction term is appreciable at large  $k_F$ , a feature that stems from the difference in the amplitude of the wave function near zero separation via the induced two-body force. At small  $k_F$ , the expectation values of the induced two and three- $\alpha$  interactions become positive, where the magnitude of the repulsive induced three- $\alpha$  interaction is larger than that of the induced two- $\alpha$  interaction. This confirms why we do not find any stable Hoyle state for the OCM result with  $k_F = 0.036 \text{ fm}^{-1}$ .

The decomposition in the absence of the induced two- and three-body interactions is also plotted in Figs. 5 (a) and (b) as denoted by  $M^*$ . We see that both the kinetic and direct interaction terms almost follow the full calculations. Since the contributions from the induced interactions are minor, i.e., one order of magnitude smaller than the expectation values of the kinetic and direct interaction terms, the  $k_F$  dependence is predominantly determined by the Hamiltonian in the absence of the medium effects except the effective mass correction. The modeling of the  $\alpha$  cluster structure is more essential than

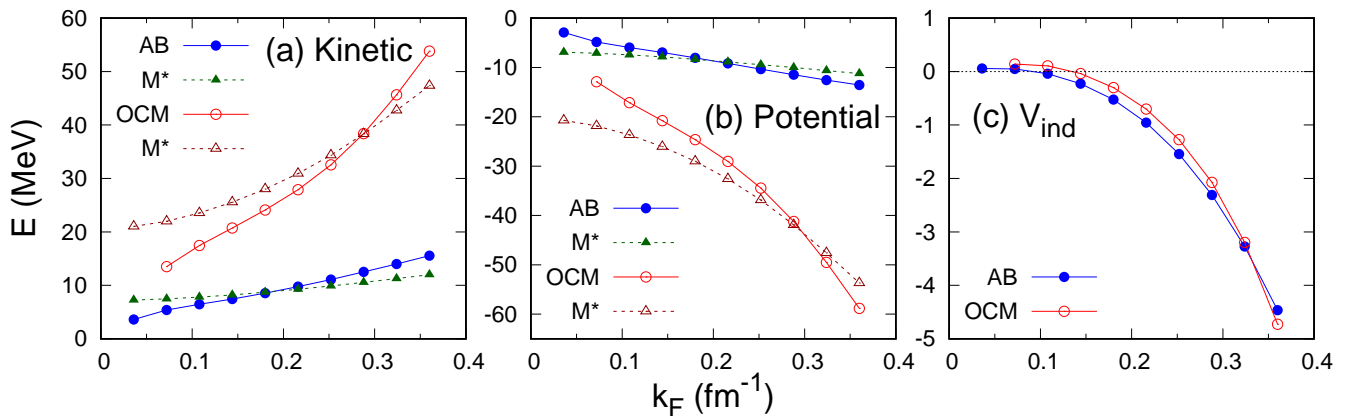


FIG. 5. Decomposition of the total three- $\alpha$  energy into the kinetic term (a), the direct potential term (b), and the induced interaction term (c), which are calculated with AB and OCM as a function of the neutron Fermi momentum. See text for details. The thin horizontal line in the panel (c) indicates zero.

the medium-induced interactions to describe the  $k_F$  dependence of the properties of the three- $\alpha$  system in cold neutron matter.

In the present study, the two- and three- $\alpha$  systems, once being bound, have an infinitely long lifetime. This is because we have assumed that each  $\alpha$  particle is robust in dilute, cold neutron medium and that possible medium effects come into our calculations only through the effective mass and in-medium interactions. In order to evaluate the lifetime of the two- and three- $\alpha$  bound states in the present cluster picture, we have to take into account a multiple scattering process among  $\alpha$  particles and surrounding neutrons, e.g., in few-body T-matrix approach. Such a process has not been considered in the present study. We expect, however, that the resultant width (the inverse lifetime) of these bound states would be negligibly small compared to the in-medium energy shift of each  $\alpha$  particle, because, as was found in Ref. [8], the decay process from a single polaronic  $\alpha$  particle to a bare  $\alpha$  particle and neutrons is kinematically suppressed due to the neutron Fermi degeneracy at low temperature. We expect that a similar mechanism works also for the two- and three- $\alpha$  particle systems; the broadening is not so large as to lose the cluster picture.

#### IV. CONCLUSION AND FUTURE PROSPECTIVE

The possibility that normally resonant two- and three- $\alpha$  systems become bound in cold neutron matter has been pointed out for the first time by combining precise quantum-mechanical calculations with a polaron picture of  $\alpha$  particles. We have examined two standard  $\alpha$ -cluster models that take into account the Pauli principle in a different way, i.e., via the Pauli potential and the orthogonality condition to the Pauli forbidden bound states. We have shown that the ground state of  ${}^8\text{Be}$  and the

Hoyle state can be bound at  $k_F \gtrsim 0.08\text{--}0.11 \text{ fm}^{-1}$  and  $k_F \gtrsim 0.16\text{--}0.22 \text{ fm}^{-1}$ , respectively, for the two models. The presence of these light nuclear ingredients as bound states would give a significant impact on the modeling of matter in stellar collapse and neutron star mergers and also affect reaction rates for nucleosynthesis therein.

It is interesting to note that the in-medium attraction discussed in this work has to be realized in finite nuclear systems, e.g., Be and C isotopes, where the  $\alpha$  cluster structure is well developed. See, e.g., Ref. [70] and references therein. Isotope dependence of the structure of  $2\alpha + Xn$  and  $3\alpha + Xn$  systems would drop a hint at the stability of  $\alpha$  clusters in cold neutron matter. As this is just the first evaluation, for simplicity, we ignore the distortion of an  $\alpha$  particle and the Pauli constraint of the relative wave function of  $\alpha$  particles by the surrounding neutron matter. The latter contribution would work as repulsion and might counteract the stability of the ‘bound’  ${}^8\text{Be}$  and Hoyle states. It would be desired to develop a model that includes such explicit correlations from the neutron medium by starting from the nucleon degrees of freedom.

Moreover, finite temperature effects would be important in core-collapse supernovae and neutron star mergers. Although we use the zero-temperature results for in-medium excitation properties of a single  $\alpha$  particle and induced two- and three- $\alpha$  interactions, the description of such in-medium properties can be extended to the finite-temperature case along the theoretical developments in cold atom physics [71–73]. Works in these directions are underway and will be reported elsewhere.

#### ACKNOWLEDGMENTS

This work was in part supported by JSPS KAKENHI Nos. 17K05445, 18K03635, 18H01211, 18H04569, 18H05406, and 19H05140, and the Collaborative Re-



- 
- [1] K. Ikeda, N. Takigawa, and H. Horiuchi, *Prog. Theor. Phys. Suppl.* **E68**, 464 (1968)
- [2] F. Hoyle, *Astrophys. J. Suppl. Ser.* **1**, 12 (1954).
- [3] E. E. Salpeter, *Astrophys. J.* **115**, 326 (1952).
- [4] M. Oertel, M. Hempel, T. Klähn, and S. Typel, *Rev. Mod. Phys.* **89**, 015007 (2017).
- [5] B. P. Abbott *et al.* (LIGO Scientific Collaboration and Virgo Collaboration), *Phys. Rev. Lett.* **119**, 161101 (2017).
- [6] M. Hempel, J. Schaffner-Bielich, S. Typel, and G. Röpke, *Phys. Rev. C* **84**, 055804 (2011).
- [7] J. Tanaka, Z. H. Yang, S. Typel, S. Adachi, S. Bai, P. van Beek, D. Beumel, Y. Fujikawa, J. Han, S. Heil *et al.*, *Science* **371**, 260 (2021).
- [8] E. Nakano, K. Iida, and W. Horiuchi, *Phys. Rev. C* **102**, 055802 (2020).
- [9] G. Röpke, *Phys. Rev. C* **101**, 064310 (2020).
- [10] F. Chevy and C. Mora, *Rep. Prog. Phys.* **73**, 112401 (2010).
- [11] P. Massignan, M. Zaccanti, and G. M. Bruun, *Rep. Prog. Phys.* **77**, 034401 (2014).
- [12] R. Schmidt, M. Knap, D. A. Ivanov, J.-S. You, M. Cetina, and E. Demler, *Rep. Prog. Phys.* **81**, 024401 (2018).
- [13] A. Schirotzek, C.-H. Wu, A. Sommer, and M. W. Zwierlein, *Phys. Rev. Lett.* **102**, 230402 (2009).
- [14] S. Nascimbène, N. Navon, K. J. Jiang, L. Tarruell, M. Teichmann, J. McKeever, F. Chevy, and C. Salomon, *Phys. Rev. Lett.* **103**, 170402 (2009).
- [15] A. Sommer, M. Ku and M. W. Zwierlein, *New J. Phys.* **13**, 055009 (2011).
- [16] C. Kohstall, M. Zaccanti, M. Jag, A. Trenkwalder, P. Massignan, G. M. Bruun, F. Schreck, and R. Grimm, *Nature* **485**, 615 (2012).
- [17] M. Cetina, M. Jag, R. S. Lous, I. Fritsche, J. T. M. Walraven, R. Grimm, J. Levinsen, M. M. Parish, R. Schmidt, M. Knap, E. Demler, *Science* **354**, 96 (2016).
- [18] F. Scazza, G. Valtolina, P. Massignan, A. Recati, A. Amico, A. Burchianti, C. Fort, M. Inguscio, M. Zaccanti, and G. Roati *Phys. Rev. Lett.* **118**, 083602 (2017).
- [19] Z. Yan, P. B. Patel, B. Mukherjee, R. J. Fletcher, J. Struck, and M. W. Zwierlein, *Phys. Rev. Lett.* **122**, 093401 (2019).
- [20] G. Ness, C. Shkedrov, Y. Florshaim, O. K. Diessel, J. von Milczewski, R. Schmidt, and Y. Sagi, *Phys. Rev. X* **10**, 041019 (2020).
- [21] I. Fritsche, C. Baroni, E. Dobler, E. Kirilov, B. Huang, R. Grimm, G. M. Bruun, P. Massignan, *Phys. Rev. A* **103**, 053314 (2021).
- [22] F. Chevy, *Phys. Rev. A* **74**, 063628 (2006).
- [23] R. Combescot, A. Recati, C. Lobo, and F. Chevy, *Phys. Rev. Lett.* **98**, 180402 (2007).
- [24] B. J. DeSalvo, K. Patel, G. Cai, and C. Chin, *Nature* **568**, 61 (2019).
- [25] H. Edri, B. Raz, N. Matzliah, N. Davidson, and R. Ozeri, *Phys. Rev. Lett.* **124**, 163401 (2020).
- [26] K. R. Patton and D. E. Sheehy, *Phys. Rev. A* **83**, 051607(R) (2011).
- [27] A. L. Fetter, and J. D. Walecka, *Quantum Theory of Many-Particle Systems*, (Dover, New York, 2003).
- [28] J. H. Van Vleck, *Rev. Mod. Phys.* **34**, 682 (1962).
- [29] Y. Nishida, *Phys. Rev. A* **79**, 013629 (2009).
- [30] S. De and I. B. Spielman, *App. Phys. B* **114**, 527 (2014).
- [31] D. Suchet, Z. Wu, F. Chevy, and G. M. Bruun, *Phys. Rev. A* **95**, 043643 (2017).
- [32] R. Liao, *Phys. Rev. Res.* **2**, 043218 (2020).
- [33] H. Tajima, J. Takahashi, S. I. Mistakidis, E. Nakano, and K. Iida, *Atoms* **9**, 18 (2021).
- [34] E. C. Pinilla, D. Baye, P. Descouvemont, W. Horiuchi, and Y. Suzuki, *Nucl. Phys. A* **865**, 43 (2011).
- [35] T. Arai, W. Horiuchi, and D. Baye, *Nucl. Phys. A* **977**, 82 (2018).
- [36] H. Moriya, W. Horiuchi, J. Casal, and L. Fortunato, *Few-Body Syst.* **62**, 46 (2021).
- [37] S. Ali and A. R. Bodmer, *Nucl. Phys.* **80**, 99 (1966).
- [38] D. V. Fedorov and A. S. Jensen, *Phys. Lett. B* **389**, 631 (1996).
- [39] D. R. Tilley, J. H. Kelley, J. L. Godwin, D. J. Millener, J. E. Purcell, C. G. Sheu, H. R. Weller, *Nucl. Phys. A* **745**, 155 (2004).
- [40] Y. Suzuki and M. Takahashi, *Phys. Rev. C* **65**, 064318 (2002).
- [41] S. Ishikawa, *Phys. Rev. C* **87**, 055804 (2013).
- [42] K. Ogata, M. Kan, and K. Kamimura, *Prog. Theor. Phys.* **122**, 1055 (2009).
- [43] N. B. Nguyen, F. M. Nunes, I. J. Thompson, and E. F. Brown, *Phys. Rev. Lett.* **109**, 141101 (2012).
- [44] T. Akahori, Y. Funaki, and K. Yabana, *Phys. Rev. C* **92**, 022801(R) (2015).
- [45] H. Suno, Y. Suzuki, and P. Descouvemont, *Phys. Rev. C* **94**, 054607 (2016).
- [46] Lai Hnin Phyu, H. Moriya, W. Horiuchi, K. Iida, K. Noda, and M. T. Yamashita, *Prog. Theor. Exp. Phys.* **2020**, 093D01 (2020).
- [47] Lai Hnin Phyu, H. Moriya, W. Horiuchi, K. Iida, K. Noda, and M. T. Yamashita, *Few-Body Syst.* **62**, 44 (2021).
- [48] F. Ajzenberg-Selove, *Nucl. Phys. A* **506**, 1 (1990).
- [49] S. Saito, *Prog. Theor. Phys.* **40**, 893 (1968).
- [50] S. Saito, *Prog. Theor. Phys.* **41**, 705 (1969).
- [51] S. Saito, *Prog. Theor. Phys.* **62**, 11 (1977).
- [52] T. Yamada and P. Schuck, *Eur. Phys. J A* **26**, 185 (2005).
- [53] Y. Funaki, T. Yamada, H. Horiuchi, G. Röpke, P. Schuck, and A. Tohsaki, *Phys. Rev. Lett.* **101**, 082502 (2008).
- [54] E. W. Schmid and K. Wildermuth, *Nucl. Phys.* **26**, 463 (1961).
- [55] K. Fukatsu and K. Katō, *Prog. Theor. Phys.* **87**, 151 (1992).
- [56] C. Kurokawa and K. Katō, *Phys. Rev. C* **71**, 021301(R) (2005).
- [57] C. Kurokawa and K. Katō, *Nucl. Phys. A* **792**, 82 (2007).
- [58] S. Ohtsubo, Y. Fukushima, M. Kamimura, and E. Hiyama, *Prog. Theor. Exp. Phys.* **2013**, 073D02 (2013).
- [59] K. Varga and Y. Suzuki, *Phys. Rev. C* **52**, 2885 (1995).
- [60] Y. Suzuki and K. Varga, *Stochastic Variational Approach to Quantum-Mechanical Few-Body Problems*, Lec-

- ture Notes in Physics, Vol. m54 (Springer, Berlin, 1998).
- [61] Y. Suzuki, W. Horiuchi, M. Orabi, and K. Arai, *Few-Body Syst.* **42**, 33 (2008).
- [62] W. Horiuchi and Y. Suzuki, *Phys. Rev. C* **78**, 034305 (2008).
- [63] W. Horiuchi and Y. Suzuki, *Few-Body Syst.* **54**, 2407 (2013).
- [64] W. Horiuchi and Y. Suzuki, *Phys. Rev. C* **87**, 034001 (2013).
- [65] J. Mitroy, S. Bubin, W. Horiuchi, Y. Suzuki, L. Adamowicz, W. Cencek, K. Szalewicz, J. Komasa, D. Blume, and K. Varga, *Rev. Mod. Phys.* **85**, 693 (2013).
- [66] Y. Suzuki and W. Horiuchi, *Emergent Phenomena in Atomic Nuclei from Large-scale Modeling: A Symmetry-Guided Perspective* (World Scientific, Singapore, 2017), Chap. 7, pp. 199-227.
- [67] V. I. Kukulin and V. N. Pomenertsev, *Ann. Phys. (New York)* **111**, 330 (1978).
- [68] M. Lyu, Z. Ren, B. Zhou, Y. Funaki, H. Horiuchi, G. Röpke, P. Schuck, A. Tohsaki, C. Xu, and T. Yamada, *Phys. Rev. C* **91**, 014313 (2015).
- [69] G. Röpke, *Phys. Rev. C* **79**, 014002 (2009).
- [70] Y. Kanada-En'yo, *Phys. Rev. C* **91**, 014315 (2015).
- [71] H. Hu, B. C. Mulkerin, J. Wang, and X.-J. Liu, *Phys. Rev. A* **98**, 013626 (2018).
- [72] H. Tajima and S. Uchino, *New J. Phys.* **20**, 073048 (2018).
- [73] W. E. Liu, J. Levinsen, and M. M. Parish, *Phys. Rev. Lett.* **122**, 205301 (2019).